KSME Journal, Vol.5, No.2, pp. 71~78, 1991

TRANSIENT RESPONSE ANALYSIS OF AN ELECTRET MICROPHONE

Whang Cho*

(*Received February 18, 1991*)

The transient response of an electret microphone without a back cavity (i.e., with no cavity below the back electrode which communicates with the air trapped between the foil and the back electrode) is analyzed by examining the motion of the electret foil in response to a transient acoustic signal applied uniformly on the foil face. The analysis uses a normal mode expansion of the motion of the circular diaphragm. A numerical evaluation of the time domain response of the electret microphone based on the analysis is pressented for the acoustic excitation by an N-wave(i.e., shock wave). Results for the N-wave show good agreement with experimental measurements, both in motion of membrane and output voltage.

Key Words: Electret Foil Microphone, Acoustic Signal, Radiation Impedance, N-wave, Integro-Differential Equation

1. INTRODUCTION

Since the behavior of foil electret transducers was first introduced by Sessler and West (1962), there has been rapid progress in electret applications. The major application which has ensued is the electret microphone. A review of the development of the foil electret microphone may be found in papers by Sessler and West (1973) and Sessler (1980).

Although electret foil microphones have been recognized as having an ability to provide flat frequency resp onse, low distortion, and low vibration sensitivity without requiring an external DC bias, and have been used to record high frequency signals, little theoretical work has been done on the transient behavior of the electret foil microphone. Qualitative assessments have suggested that the electret microphone gives more "crisp" recording results but the assessments have not been physically explained yet. With this strong motivation, this paper will analyze theoretically the transient behavior of a geometrically rather simple type of electret foil microphone.

The solution process of the problem at hand can be divided into two parts: finding the static deflection of the electret membrane and finding the dynamic deflection. For the static part of the solution direct use of the results given by Busch-Vishniac (1984) was made. This implies that major portion of this paper will be devoted to finding the dynamic behavior.

Since the transient motion of the electret foil of a microphone depends upon the initial static deflection, which is due to electrostatic forces on the membrane and is well described by a linear partial integro-differential equation, approximate solutions of this equation are obtained first for the electret microphone whose circular membrane is assumed to be held clamped at its edge. These solutions are then used to find a nonlinear partial integro-differential equation for the dynamic membrane motion. Finally, an approximate solution for the motion of the membrane is found by linearizing the motion equation and applying an operational calculus technique. Resulting output voltage is also found as a function of average displacement of membrane.

*Department of Control and Measurement Kwangwoon University, Seoul 139-050, Korea

2. MODEL OF SYSTEM

Figure 1 shows the microphone model used in the analysis. It consists of a foil electret under tension held above the rigid backplate by a ridge of height Y_o at radius $r=a$. Behind the backplate is an air gap of volume v. As shown in Fig. 1 the deflection is toward the backplate. The deflection $Y(r, t)$ is measured from undeflected position of the foil electret.

The configuration shown in Fig. 1 is a simplified version of usual microphone system in a sense that the back cavity and, therefore, the holes connecting air gap and back cavity are absent. The back chamber and connecting holes allow a real system to be more sensitive and more stable by reducing the stiffness reaction of the small air gap and by providing additional viscous damping. Note that a system with back cavity generally results in narrower bandwidth. A steady state analysis of an electret mictrophone with back cavity may be found in Zahn (1981), Petritskaya (1966, 1968), and Zuckerwar(1978).

The air gap between the foil electret and the backplate is assumed to behave as a pure stiffness under adiabatic(1) change. This is a very good approximation up to quite high frequency range, as high as about 200 Khz(refer to Kinsler (1982) and Berenak (1954)) because the depth of the air gap under consideration is very small (about 25.4×10^{-3}cm).

The foil electret is assumed to be under isotropic tension which remains constant as the foil moves and will be valid as long as the deflection of the foil is very small. Typical

(1) The air in the gap could have been assumed to be under isothermal conditions because the surface-to-volume ratio is so large that heat transfer should be efficient. But because the frequency range dealt here are greater than 3Khs, the half period is not long enough for much heat transfer to take place.

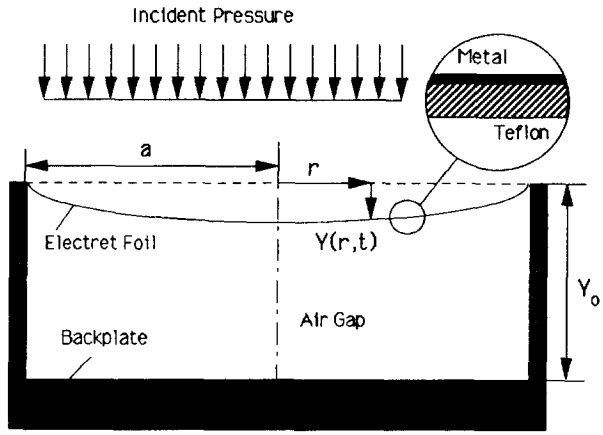

Fig. 1 Model of electret microphone

deflections are of the order of 10^{-7}cm. Also, the bending stiffness of the foil is neglected in comparison with the tension force of the membrane. For typical foil electrets using Teflon this assumption is accurate because the electrets are extremely thin (under 75×10^{-4}cm in thickness).

There are six possible sources of forces which affect the motion of the membrane: inertia, tension, incident pressure, air gap stiffness, damping due to interaction of membrane with neighboring air, and electrostatic forces. Some of these will be considered in details in the following.

First, consdier the construction of the air gap stiffness. For an adiabatic change of a gas

$$pv^{\gamma}=constant, \tag{1}$$

where p is the pressure, v the volume, and γ the ratio of specific heat at constant pressure to specific constant volume ($\gamma=1.4$ for air). A differential change of pressure due to differential volumetric change is thus

$$\Delta p=-\frac{p_o\gamma}{v_o}\Delta v, \tag{2}$$

where p_o and v_o are equilibrium values. The volumetric change of the air gap in the microphone results from foil motion.

$$\Delta v=\int_0^{2\pi}\int_0^a Y_d(r,\ t)\ rdrd\theta, \tag{3}$$

where $Y_d(r,\ t)$ denotes dynamic deflection of the electret foil in excess of static deflection $Y_s(r)$. The resulting restoring force per unit area provided by the air gap may be written as

$$f_{gap}=-\frac{p_o\gamma}{v_o}\int_0^{2\pi}\int_0^a Y_d(r,\ t)\ rdrd\theta, \tag{4}$$

where f_{gap} is negative if deflection is positive (i.e., downward) and vice versa.

Next consider the electrostatic force per unit area on the foil. Sessler (1980) has shown that this force is given by

$$f_{electrostatic}=-\frac{(s\sigma+\varepsilon\varepsilon_o V)^2}{2\varepsilon_o(s+\varepsilon Y_o+\varepsilon Y_s+\varepsilon Y_d)^2} \tag{5}$$

where s is the foil thickness in cm, σ is the charge density in esu/cm^2, ε is the dielectric constant of polymer ($\varepsilon=2.1$ for Teflon), and V is the output voltage in volts. Note that this force is a function of radial location and time because $Y_s=Y_s(r)$ and $Y_d=Y_d(r,\ t)$.

Now consider the damping force on the foil electret. Once the foil is excited by an incident sound wave and starts to vibrate, the foil pushes the neighboring air layer back and forth, giving some energy back to the space. This mechanism of energy loss is neglected for most vibration analysis because the vibrating object usually has a much larger mass than that of neighboring air layer, but here this is not the case.

The mass of the foil is so small that this energy loss can not be neglected. The mechanism of this energy transfer is well defined in acoustical terminology by the radiation impedance of a foil. Exact derivation of the radiation impedance of an arbitrarily moving circular membrane is very involved and not pursued here. Instead, actual impedance is approximated by the counterpart of rigid circular piston in an infinite baffle. The assumption under which this approximation can be justified is that the velocity of sound in the surrounding fluid (air in this case) is much greater than the wave propagation velocity in the membrane. If this assumption holds, the membrane hardly feels the pressure difference between any two points on its face due to fast compensation by sound propagation. A more detailed discussion on this subject is given in Morse and Ingard(1968).

The well known formula for specific acoustic radiation impedance ($=p/u$ where p=pressure and u=velocity) of a circular rigid piston in an infinite baffle is given by (see Morse and Ingard (1968))

$$Z(\omega)=\theta_o+iX_o \tag{6}$$

where

$$\theta_o=\rho c\left\{1-\frac{2}{w}J_1(w)\right\}, \tag{7}$$

$$X_o=\rho c\left[\frac{2}{\pi}\int_0^{\pi}\sin\ (w\cdot\cos\ (\alpha))\cdot\sin^2(\alpha)\,d\alpha\right], \tag{8}$$

$i=\sqrt{-1}$, $w=2\omega a/c$, ρ the density of air, c the sound velocity in air, J_1 the first order Bessel function, ω the radian frequency, and a the radius of the piston. The real part of $Z(w)$ is called the radiation resistance and causes the system to dissipate energy. The imaginary part is called the radiation reactance and explains the air loading effect on the piston during the motion. Note that even in this case of foil vibration the mass loading effect can be neglected because it is orders of magnitude less than the mass reactance of the foil. In fact at sufficiently high frequency the impedance becomes purely resistive(see Morse and Ingard (1968)). From Eq. (6), the damping force per unit area on themembrane is

$$f_{damping}=\theta_o\left(\frac{1}{\pi a^2}\int_0^{2\pi}\int_0^a\frac{\partial Y_d}{\partial t}\right) \tag{9}$$

The expression in the parentheses gives the average velocity of the foil at a given time.

In addition to the energy dissipation associated with radiation, thre is energy loss due to "sloshing" of air trapped in the air gap. However, this energy loss may be easily argued to be small enough to be neglected. Since the gap may be modeled as a very short closed cavity, inside pressure is approximately uniform thereby implying negligible particle velocity. With

no particle velocity, the sloshing loss would be zero. Another energy loss mechanism due to heat transfer, which would have a rather larger effect than air aloshing, is also englected.

Finally taking the restoring force of the foil due to tension into account, the following motion equation of the foil is obtained.

$$\rho_s\frac{\partial^2 Y_d}{\partial t^2}+\frac{p_o\gamma}{v_o}\int_0^{2\pi}\int_0^a Y_d\ rdrd\theta + \frac{\theta_o(\omega)}{\pi a^2}\int_0^{2\pi}\int_0^a\frac{\partial Y_d}{\partial t}rdrd\theta - T\nabla^2(Y_d+Y_s) = -P-\frac{(s\sigma+\varepsilon\varepsilon_o V)^2}{2\varepsilon_o(s+\varepsilon Y_o+\varepsilon Y_s+\varepsilon Y_d)^2} \tag{10}$$

where ρ_s, is the mass of the foil per unit area, $\theta_o(\omega)$ the real part of the radiation impedance, P the applied pressure, T the tension of the foil, and ∇^2 the Laplacian operator in radial coordinate.

By setting $Y_d=0$, $V=0$, and $P=0$, the static force balance equation can be obtained from Eq. (10) as

$$T\nabla^2 Y_s=-\frac{(s\sigma+\varepsilon\varepsilon_o V)^2}{2\varepsilon_o(s+\varepsilon Y_o+\varepsilon Y_s)^2} \tag{11}$$

Note that this equation is highly nonlinear. The nonlinearity may cause an instability. If Y_s is sufficiently small, stable deflection results. If Y_s is not small enough, the tension may not hold the foil up and let it collapse onto the back electrode. As mentioned earlier, an approximate solution to this static deflection equation was found analytically by Busch-Vishniac (1984) by using a power series expansion. Results show that the static deflection can be approximated to a high degreee of accuracy by a parabolic curve. There, it was also shown that for stable deflection the ratio of the maximum amplitude (Y_s at the center) to Y_o must be of order of 10^{-3} or less.

Since Eq. (10) is very difficult to solve directly, some careful simplification is necessary as follows. First, the numerator of the second term on the right hand side of Eq. (10) is expanded to get

$$\rho_s\frac{\partial^2 Y_d}{\partial t^2}+\frac{p_o\gamma}{v_o}\int_0^{2\pi}\int_0^a Y_d\ rdrd\theta+\frac{\theta_o(\omega)}{\pi a^2}\int_0^{2\pi}\int_0^a\frac{\partial Y_d}{\partial t}rdrd\theta = -P+T\nabla^2(Y_d+Y_s)-\frac{s^2\sigma^2(\varepsilon\varepsilon_o V/s\sigma)}{\varepsilon_o(s+\varepsilon Y_o+\varepsilon Y_s+\varepsilon Y_d)^2} - \frac{s^2\sigma^2}{2\varepsilon_o(s+\varepsilon Y_o+\varepsilon Y_s+\varepsilon Y_d)^2}-\frac{s^2\sigma^2(\varepsilon\varepsilon_o V/s\sigma)^2}{2\varepsilon_o(s+\varepsilon Y_o+\varepsilon Y_s+\varepsilon Y_d)^2} \tag{12}$$

Expanding the denominator by assuming $|Y_d/Y_o|\ll|Y_s/Y_o|$ and keeping the first order terms only, the DC electrostatic term becomes

$$-\frac{s^2\sigma^2}{2\varepsilon_o(s+\varepsilon Y_o+\varepsilon Y_s+\varepsilon Y_d)^2} \approx -\frac{s^2\sigma^2}{2\varepsilon_o(s+\varepsilon Y_o+\varepsilon Y_s)^2}+\frac{s^2\sigma^2\varepsilon Y_d}{2\varepsilon_o(s+\varepsilon Y_o+\varepsilon Y_s)^3} \tag{13}$$

The first of these two terms balances the term $T\nabla^2 Y_s$. The last term in Eq. (12) shows the distortion effect due to the nonlinear dependence on voltage and may be neglected because it depends only on a small term of second order $(\varepsilon\varepsilon_o/s\sigma)^2 V$ with $s\sigma/\varepsilon\varepsilon_o$ being 300 volts of DC potential and V the output AC voltage of order of milivolts. The remaining electrostatic ferm is approximated as

$$-\frac{s^2\sigma^2(\varepsilon\varepsilon_o V/s\sigma)}{\varepsilon_o(s+\varepsilon Y_o+\varepsilon Y_s+\varepsilon Y_d)^2}\simeq-\frac{s^2\sigma^2(\varepsilon\varepsilon_o V/s\sigma)}{\varepsilon_o(s+\varepsilon Y_o+\varepsilon Y_s)^2}.$$

$$\left\{1-\frac{2\varepsilon Y_d}{s+\varepsilon Y_o+\varepsilon Y_s}+\cdots\right\}\approx\frac{s\sigma\varepsilon V}{(s+\varepsilon Y_o+\varepsilon Y_s)^2} \tag{14}$$

What remains is to relate the output voltage V to the motion of foil electret Y_d. Sessler (1980) showed that

$$V=\frac{s\sigma Y_d}{\varepsilon_o(s+\varepsilon Y_o+\varepsilon Y_s+\varepsilon Y_d)} \tag{15}$$

by assuming piston-like motion of the foil. A plausible extension of this result can be made by using the average displacement of the foil instead of assuming a uniform piston-like displacement for Y_d in Eq. (15). This leads to

$$V=\frac{s\sigma}{\pi a^2\varepsilon_o}\int_0^{2\pi}\int_0^a\frac{Y_d}{s+\varepsilon Y_o+\varepsilon Y_s+\varepsilon Y_d}rdrd\theta \tag{16}$$

and again under the assumption of $|Y_d/Y_o|\ll|Y_s/Y_o|$, Eq. (16) is reduced to

$$V=\frac{s\sigma}{\pi a^2\varepsilon_o}\int_0^{2\pi}\int_0^a\frac{Y_d}{s+\varepsilon Y_o+\varepsilon Y_s}rdrd\theta \tag{17}$$

Finally putting terms all together, the motion equation of the foil is written as

$$\rho_s\frac{\partial^2 Y_d}{\partial t^2}+\frac{p_o\gamma}{v_o}\int_0^{2\pi}\int_0^a Y_d\ rdrd\theta+\frac{\theta_o(\omega)}{\pi a^2}\int_0^{2\pi}\int_0^a\frac{\partial Y_d}{\partial t}rdrd\theta + \frac{(s\sigma)^2\varepsilon}{\pi a^2\varepsilon_o(s+\varepsilon Y_o+\varepsilon Y_s)^2}\int_0^{2\pi}\int_0^a\frac{Y_d}{s+\varepsilon Y_o+\varepsilon Y_s}rdrd\theta - T\nabla^2 Y_d-\frac{(s\sigma)^2\varepsilon}{\varepsilon_o(s+\varepsilon Y_o+\varepsilon Y_s)^3}Y_d=-P \tag{18}$$

This is linear partial integro-differential equation. Finally, introducting a nondimensional radial coordinate $\delta=r/a$ and simplifying the denominator under the assumption of $|Y_d|\ll|Y_s|$ yield

$$\rho_s\frac{\partial^2 Y_d}{\partial t^2}+\frac{p_o\gamma a^2}{v_o}\int_0^{2\pi}\int_0^1 Y_d\delta d\delta d\theta+\frac{\theta_o(\omega)}{\pi}\int_0^{2\pi}\int_0^1\frac{\partial Y_d}{\partial t}\delta d\delta d\theta + \frac{(s\sigma)^2\varepsilon}{\varepsilon_o(s+\varepsilon Y_o)^3}\int_0^{2\pi}\int_0^1 Y_d\delta d\delta d\theta-\frac{T}{a^2}\nabla^2 Y_d - \frac{(s\sigma)^2\varepsilon}{\varepsilon_o(s+\varepsilon Y_o+\varepsilon Y_s)^3}Y_d=-P \tag{19}$$

where

$$\nabla^2=\frac{\partial}{\delta\partial\delta}\left(\delta\frac{\partial}{\partial\delta}\right) \tag{20}$$

Note that Eq. (19) is linear in Y_d linear in Y_d and no longer shows dependence on Y_s. In other words, to the leading order, the dynamic deflection of the foil is independent of the static deflection.

There exist two boundary conditions which constrain the motion of the foil at the ridge and at the center of the foil. No deflection at the ridge implies

$$Y_d(\delta=1,\ t)=0 \tag{21}$$

and stable deflection at the center of the foil gives

$$Y_d(\delta=0,\ t)=bounded \tag{22}$$

The initial condition is chosen to be that of no motion and no deformation, and may be expressed as follows :

$$\frac{\partial}{\partial t}\{Y_d(\delta,\ t=0)\}=0, \tag{23}$$

and

$$Y_d(\delta,\ t=0)=0 \tag{24}$$

Equations (19) and (21) through (24) ocmpose a mathematically well posed problem and their solution will be sought in the following section.

3. ANALYSIS

There may be many ways to solve Eq. (19). Here, operational calculus technique will be used. One of the advantages of using this technique is that it allows a closed form solution. When it is necessary to choose optimum system parameters, say, radius, ridge height, and tension of the microphone, etc, then a power series expansion method may be a better choice for attacking this problem analytically. A power series approach, however, would require many terms for results with required accuracy.

The first step in solving Eq. (19) is to assume the proper form of the solution for a time harmonic input pressure,

$$P=P_o e^{i\omega t} \tag{25}$$

Here the simplicity and ease of analytical evaluation of the integral terms and Laplacian operator should be taken into consideration. In view of the fact that circular membranes exhibit Bessel function type solutions, and that boundedness of the solution (refer to Eq. (22)) eliminates the possible appearance of Neuman function, a reasonable form to be assumed for the solution to Eq. (19) is

$$Y_d(\delta,\ t)=A(\omega)\{J_o(a\delta k)-J_o(ak)\}e^{i\omega t} \tag{26}$$

where $A(\omega)$ is the amplitude factor which is a function of angular frequency ω, J_o the zeroth order Bessel function, and k the wave number. Note that only J_o the zeroth order Bessel function, and k the wave number. Note that only J_o terms appear because $J_i(i>0)$ give no response at the center and that only term in the parentheses is assumed to be dependent on δ. This assumption will play a role subsequently. Notice also that Eq. (26) satisfies both boundary conditions, i.e., Eqs. (21) and (22), and the initial conditions, i.e., Eqs. (23) and (24).

The next step is to determine $A(\omega)$ by substituting the assumed solution into the original motion equation. Term by term substitutions yield followings.

$$\rho_s\frac{\partial^2 Y_d}{\partial t^2}=-\omega^2 A(\omega)\{J_o(a\delta k)-J_o(ak)\}e^{i\omega t} \tag{27}$$

$$\frac{p_o\gamma a^2}{v_o}\int_0^{2\pi}\int_0^1 Y_d\delta d\delta d\theta=\frac{\rho_o\gamma a^2}{v_o}\int_0^1 A(\omega)\{J_o(a\delta k)-J_o(ak)\}e^{i\omega t}d\delta \tag{28}$$

$$=\frac{\pi p_o\gamma a^2}{v_o}A(\omega)J_2(ak)\,e^{i\omega t} \tag{29}$$

$$\frac{\theta_o(\omega)}{\pi}\int_0^{2\pi}\int_0^1\frac{\partial Y_d}{\partial t}\delta d\delta d\theta=i\omega\theta_o(\omega)A(\omega)J_2(ak)\,e^{i\omega t} \tag{30}$$

$$\frac{(s\sigma)^2\varepsilon}{\varepsilon_o(s+\varepsilon Y_o)^3}\int_0^{2\pi}\int_0^1 Y_d\ \delta d\delta d\theta$$

$$=\frac{(s\sigma)^2\varepsilon}{\varepsilon_o(s+\varepsilon Y_o)^3}A(\omega)J_2(ak)\,e^{i\omega t} \tag{31}$$

$$-\frac{T}{a^2}\nabla^2 Y_d=Tk^2A(\omega)J_o(a\delta k)\,e^{i\omega t} \tag{32}$$

Using the above results yields $A(\omega)$ as

$$A(\omega)=\frac{P_o}{\Delta} \tag{33}$$

where

$$\Delta=\left\{\frac{\pi p_o\gamma a^2}{v_o}+\frac{s^2\delta^2\varepsilon}{\varepsilon_o(s+\varepsilon Y_o)^3}+i\omega\theta_o(\omega)\right\}J_2(ak)$$
$$+\left\{Tk^2-\rho_s\omega^2-\frac{s^2\sigma^2\varepsilon}{\varepsilon_0(s+\varepsilon Y_o)^3}\right\}J_o(a\delta k)$$
$$+\left\{\rho_s\omega^2+\frac{s^2\sigma^2\varepsilon}{\varepsilon_o(s+\varepsilon Y_o)^3}\right\}J_o(ak) \tag{34}$$

The presence of the term $J_o(a\delta k)$, a function of δ, in the denominator of $A(\omega)$ violates the initial assumption that $A(\omega)$ is a function of ω only. This contradiction can be easily eliminated by properly choosing k such that the second parentheses in the denominator of $A(\omega)$ becomes zero. The wave number k so defined is given by

$$k(\omega)=\left\{\frac{\rho_s\omega^2}{T}+\frac{s^2\sigma^2\varepsilon}{T\varepsilon_o(s+\varepsilon Y_o)^3}\right\}^{1/2} \tag{35}$$

This result for k has an important physical meaning which can be seen more easily in the following expression.

$$C_m=\frac{\omega}{k} \tag{36}$$

$$=\frac{\omega}{\left\{\frac{\rho_s\omega^2}{T}+\frac{s^2\sigma^2\varepsilon}{T\varepsilon_s(s+\varepsilon Y_o)^3}\right\}^{1/2}} \tag{37}$$

where C_m is the wave propagation velocity in the membrane. Note that the wave propagation velocity in the foil is a function of ω, i.e., the motion is "dispersive". As the frequency of the wave goes to infinity, the corresp onding propagation velocity in the electret foil approaches that of a normal simple membrane, i.e., $(T/\rho_s)^{1/2}$. As frequency is reduced it propagates more slowly, becoming stationary for the pure DC component.

Now expression for $A(\omega)$ can be simplified as

$$A(\omega)=\frac{P_o}{\left\{\rho_s\omega^2+\frac{s^2\sigma^2\varepsilon}{\varepsilon_o(s+\varepsilon Y_o)^3}\right\}J_o(ak)+\left\{\frac{\pi p_o\gamma a^2}{v_o}+\frac{s^2\delta^2\varepsilon}{\varepsilon_o(s+\varepsilon Y_o)^3}+i\omega\theta_o(\omega)\right\}J_2(ak)} \tag{38}$$

Having found $A(\omega)$ and k, the original assumed solution can be expressed as

$$Y_d(\delta,\ t)=\frac{P_o\{J_o(a\delta k)-J_o(ak)\}e^{i\omega t}}{\left\{\rho_s\omega^2+\frac{s^2\sigma^2\varepsilon}{\varepsilon_o(s+\varepsilon Y_o)^3}\right\}J_o(ak)+\left\{\frac{\pi p_o\gamma a^2}{v_o}+\frac{s^2\delta^2\varepsilon}{\varepsilon_o(s+\varepsilon Y_o)^3}+i\omega\theta_o(\omega)\right\}J_2(ak)} \tag{39}$$

where k is given in Eq. (35). Let's quickly assess the meaning of Eq. (39). Equation (38) simply indicates the frequency resp onse of the electret foil microphone. The microphone system shows different response characteristics to different frequency inputs. The infinite number of resonance frequencies are determined by the pole of the expression. The response to a general transient pressure input may thus expressed as

$$Y_d(\delta, t)=\frac{1}{2\pi}\int_{-\infty}^{+\infty}\frac{Y_m(\delta, \omega)}{i\omega}e^{i\omega t}d\omega\int_{-\infty}^{+\infty}P(\tau)e^{-i\omega\tau}d\tau \tag{40}$$

where the acoustical admittance $Y_m(\delta, \omega)$ is defined as

$$Y_m(\delta, \omega)=\frac{\partial Y_d(\delta, t)/\partial t}{P(t)} \tag{41}$$

$$=\frac{i\omega\{J_o(a\delta k)-J_o(ak)\}}{\left\{\rho_s\omega^2+\frac{s^2\sigma^2\varepsilon}{\varepsilon_o(s+\varepsilon Y_o)^3}\right\}J_o(ak)+\left\{\frac{\pi p_o\gamma a^2}{v_o}+\frac{s^2\delta^2\varepsilon}{\varepsilon_o(s+\varepsilon Y_o)^3}+i\omega\theta_o(\omega)\right\}J_2(ak)} \tag{42}$$

In what follows, a numerical result is sought for an N-wave input, which is a good approximation of a spark sound, one of the most popular transient acoustic sources especially in acoustic instrument calibration. A spark is generated between two highly changed electrodes when they exchange charges through space. The electric discharge usually takes loess than 10 μsec, but the sound generated by the spark has larger duration than that of the spark (refer to Wright (1978)). Fig. 2 shows a N-waves which will be used as trasient pressure inputs in the following analysis. In reality the propagation of an N-wave sound is well explained in nonlinear acoustics theory (see Morse and Ingard (1968)). A matematical form for an N-wave is

$$P(t)=\begin{cases}-\left(\frac{P_1-P_2}{\tau}\right)t+P_1 & 0\le t\le\tau\\ 0 & \text{otherwise}\end{cases} \tag{43}$$

where τ is the duration of the N-wave. Using this expression the last integral of Eq. (39) is evaluated as

$$P(\omega)=\int_{-\infty}^{+\infty}P(\tau)e^{-i\omega t}d\tau \tag{44}$$

$$=-\frac{P_2\{\omega\tau e^{-i\omega t}-i(e^{-i\omega t}-1)\}}{i\omega^2\tau}+\frac{P_1\{\omega\tau-i(e^{-i\omega t}-1)\}}{i\omega^2\tau} \tag{45}$$

Table 1 Parameter Values of the Test Microphone

Symbol	Meaning	Value
a	radius of the electret foil	1 cm
s	thickness of the electret foil	2.5×10^{-3}cm
ε	dielectric constant of the electret foil	2.1
ε_o	permittivity of air	$1/4\pi$ volt·esu/cm
σ	charge density of electret foil	11.09 esu/cm^2
T	tension force	1×10^{-5}dyn/cm
Y_o	ridge height of the microphone	25.4×10^{-3}cm
p_o	atmospheric pressure	1.03×10^{-6}dyn/mc^2
ρ_s	density of Teflon per unit area	5.5×10^{-3}g/cm^2
γ	specific heat ratio of air	1.4
ρ	air density	1.21×10^{-3}cm
c	sound velocity in air	3.44×10^4cm/sec
v_o	volume of the air cavity	80×10^{-3}cm^3

The evaluation of Eq. (40) together with Eqs. (42) and (45) can be done numerically using residue calculus since there are no branch points even though the expression of k has a square root form. This is because J_o and J_2 are even functions. In other words, there exist only even power terms of k.

There is one double pole at $\omega=0$ which comes from the input pressure function, and infinite number of simple poles ($s_n=\omega_n+id_n$, $n=1, \ldots, \infty$) which come from system characteristic equation. In finding the poles of the system characteristics equation, a routine from IMSL (international Mathematical Subroutine Library) was used, which seems to be the one of few available subroutines. Using this routine about 70 poles (ascending order in magnitude) could be found with good accuracy. An attempt to find more than 100 poles failed because of the limit of number handling capacity of the routine. Fortunately enough, however, a calculated result for the dynamic response of the microphone using the obtained poles shows fair convergence with a summation of only 30 terms. Summation of us to 50 terms gives excellent results for the most practical purposes showing negligible error compared with that of the 70 term summation.

It can be shown that the residue at $\omega=0$ is zero (refer to Cho (1985)) and the final expression for the dynamic displacement of the foil electret is written in a condensed form as

$$Y_d(\delta, t)=2\sum_{n=1}^{\infty}\{A_n\cdot\sin(\omega_n t)+B_n\cdot\cos(\omega_n t)\}e^{-d_n t} \tag{46}$$

where A_n and B_n are the real and imaginary parts respectively of the residue of the poles s_n.

The above table shows the numerical values of the parameters of the test microphone, used in the simulation, which was actually built for the experimental purposes.

4. RESULTS

In Figs. 3, 4, and 5, the theoretically predicted microphone motions are plotted as a function of time and location for two periods of the fundamental mode. Each figure corresponds to one of the three variations in input pressure amplitudes and durations of N-wave shown in Fig. 2. Figures 6, 7, and 8 show the resulting voltage output signals calculated from these motions using Eq. (16).

Figures 3, 4, and 5 show that the center flat portion of the foil remains underformed but moves up and down following the motion of the reflected wave from the foil edge until the reflected waves reach the center. Then the center shows large amplitude deflection caused by reflected waves overlapping themselves. The initial uniform motion of the foil of the

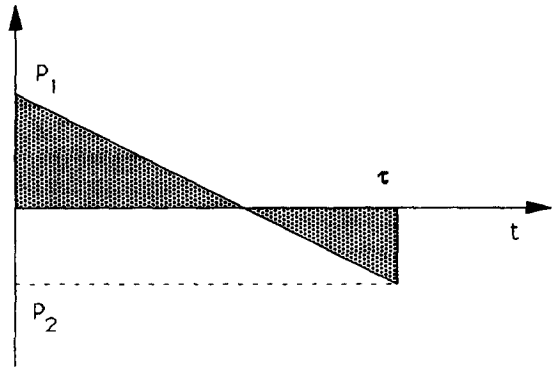

Fig. 2 Typical N-wave

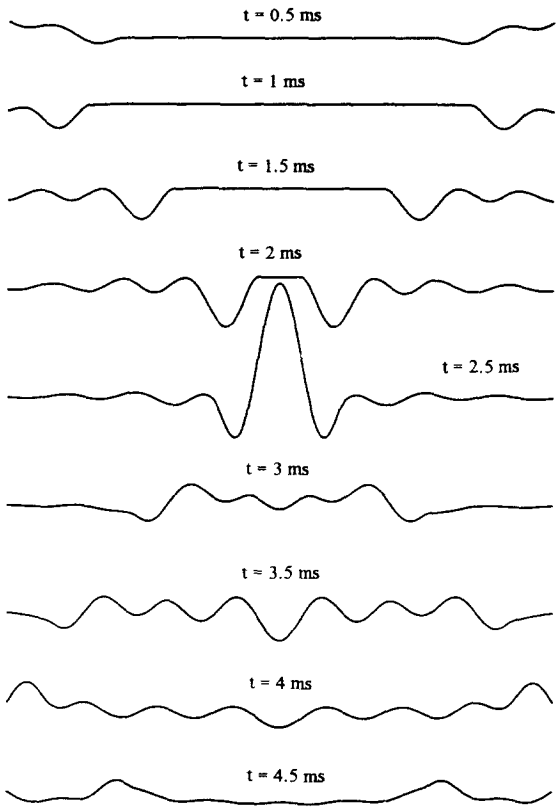

Fig. 3 $P_1=1.$, $P_2=-0.3$, $\tau=1\times10^{-4}$

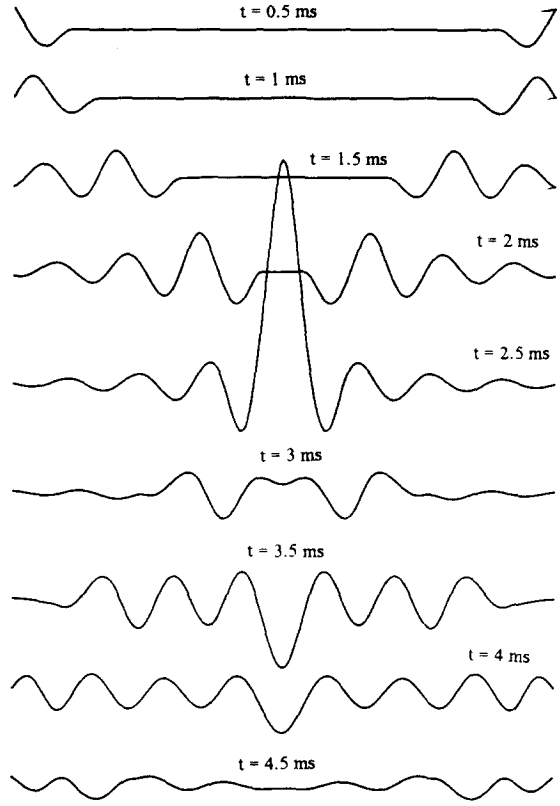

Fig. 4 $P_1=1.$, $P_2=-1.$, $\tau=1\times10^{-4}$

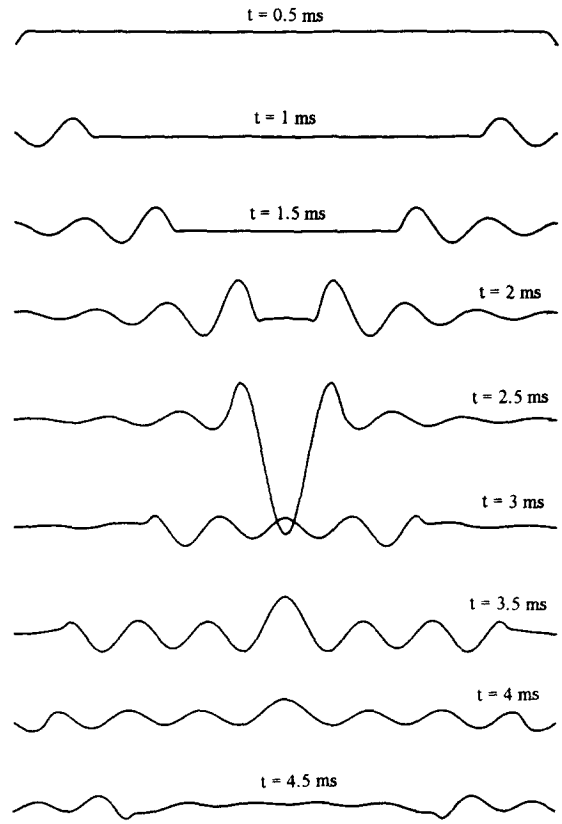

Fig. 5 $P_1=0.3$, $P_2=-1.$, $\tau=1\times10^{-4}$

microphone gives a large peak voltage which decays in amplitude as the foil oscillates. Subsequent rises in the voltage level are generated when the reflected waves are superposed at the center of the microphone foil. The interval between successive voltage packet peaks depends on the wave propagation velocity in the membrane which is not constant in this case because the system is dispersive.

Note that despite the difference in input wave form the resulting voltage outputs (Figs. 6~8) show little difference. This is because the system is highly resonant and tends to ring at the seventh resonance frequency at about 16 Khz. Every sharp change in the pressure input excites all the modes regardless of its details in the input profile but seventh mode always dominates the voltage output. In fact the damping associated with the seventh resonant mode is high relative

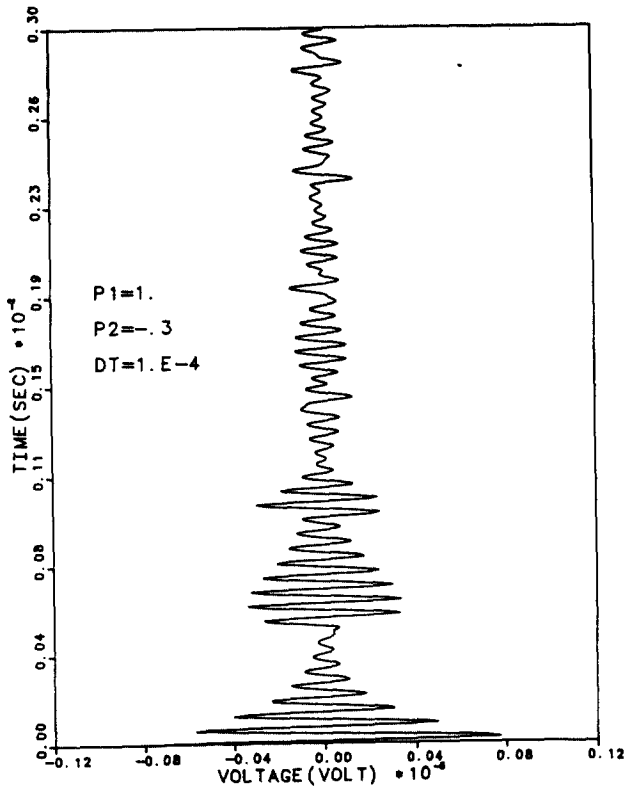

Fig. 6 Voltage output

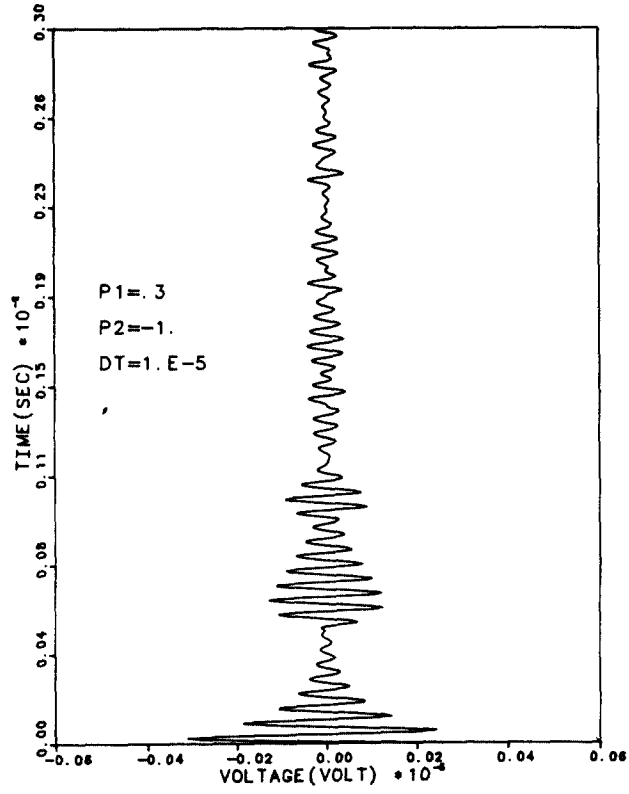

Fig. 8 Voltage output

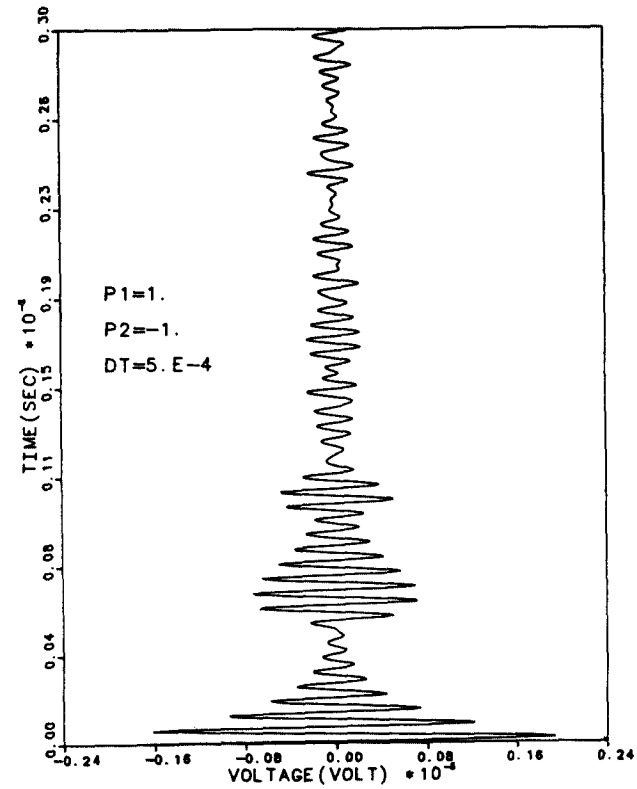

Fig. 7 Voltage output

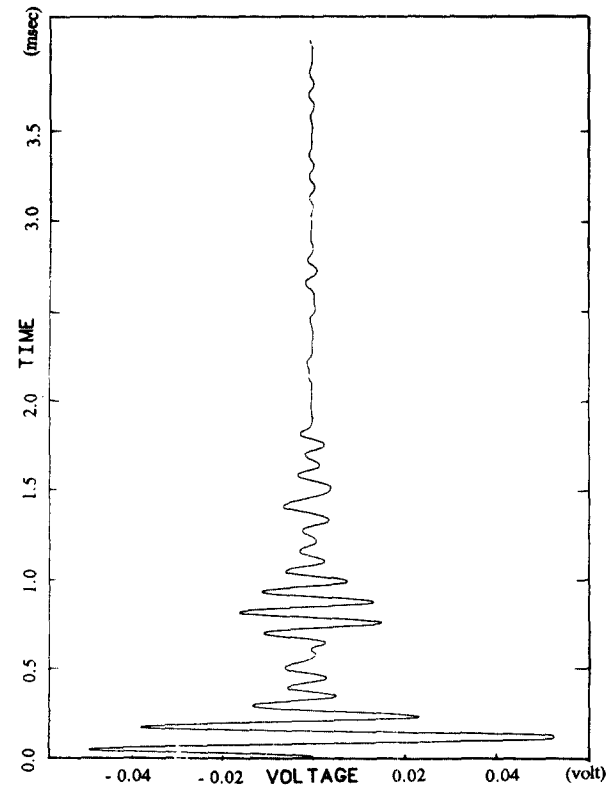

Fig. 9 Experimental voltage output

to the other modes and, therefore, even though the seventh mode initially dormionates the N-wave response, it eventually decays sufficiently that other modes become comparable in magnitude. This transition can be seen in Figs. 6 through 8 occuring at about 1.2 msec. After 1.2 msec the voltage signals clearly appear to have more than one frequency components.

The results shown in Figs. 6 through 8 may be compared with experimental results (Fig. 9) obtained in the laboratory with the test microphone. In this test a Grozier Technical System spark source was used to generate a broadband high frequency acoustic signal at the microphone face. Although it is very difficult to measure the exact shape of the acoustic pulse generated, the Grozier literature predicts an N-wave of the type shown in Fg. 2 with $P_1=P_2$ and duration of 5×10^{-5}. The same input data was used in the simulations whose results are given in Figs. 6 through 8. Hence the experimental results and predicted ones may be directly compared. The spark amplitude measured in the laboratory and hence the amplitude of the acoustic excitation was variable. As is clear from Fig. 9, the experimental results (shape) were very repeatable.

Figure 9 and Figs. 6 through 8 reveal a good similarity of signal shape but not of the amplitude decay. As the figures indicates, the real microphone exhibits a faster decay than that predicted by the analysis. This result indicates that the radiation resistance approximation made in the damping effect estimate introduces errors. As mentioned earlier, the heat transfer loss of energy should be taken into consideration for the better prediction of the transient behavior of a real microphone system.

5. CONCLUSION

Results given in previous section clearly show that both experimentally and theoretically, a circular, edge-supported electret microphone with no back cavity exhibits substantial ringing. This suggests that such a microphone is not ideal for recording transient events which contain very high frequencies. It should be noted that a conventional electret microphone has holes in the back electrode which lead to a large back cavity. This geometry will not only affect the frequency of each mode, but most likely also greatly enhance the damping of each mode. Hence the results here can not be extrapolated to a conventional electret microphone.

The success of the analytical technique opens several avenues of further investigation. Questions which remains to be answered include the following : What is the effect of adding a back cavity and passages connecting the air gap and back cavity ? What changes are necesary for treatment of non-circular electret microphones? How do these results compare to the transient response characteristics of conventional condenser microphones ?

REFERENCES

Berenak, L.L., 1954, "Acoustics," McGraw-Hill, New York

Busch-Vishniac, I., 1984, "Response of an Edge-Supported Circular Membrane Electret Earphone. Part I-Theory," J.A.S.A. 75, pp 977~987.

Cho, W., 1985, "Transient Response Analysis of Electret Microphone Without Back Cavity," Master Thesis, University of Texas at Austin.

Kinsler, L.E., Frey, A.R., Coppens, A.D. and Sanders, J.V., 1982, "Fundamentals of Acoustics," 3rd ed., John Wiley & Sons.

Morse, P.M. and Ingard, K.U., 1968, "Theoretical Acoustics," McGraw-Hill, Inc.

Petritskaya, I.G., 1966, "Impedance of a Thin Layer of Air in the Harmonic Vibration of Membrane," Soviet Physics-Acoustics 12, pp 193~198.

Petritskaya, I.G., 1968, "Vibrations of Membrane Loaded with Thin Layer of Air," Soviet Physics-Acoustics 14, pp 105~106.

Sessler, G.M. and West, J.E., 1962, "Self-Biased Condenser Microphone with High Capacitance," J.A.S.A. 34, pp 1787~1788.

Sessler, G.M. and West, J.E., 1973, "Electret Transducers : A Review," J.A.S.A. 53, pp 1589~1600.

Sessler, GM., 1980, "Electrets," Spring-Verlag, Berlin.

Wright, W.M., 1978, "Finite-Amplitude Behavior of N-shaped Pulses from Sparks," J.A.S.A 68(s1).

Zahn, R., 1981, "Analysis of the Acoustic Resp onse of Circular Electret Condenser Microphone," J.A.S.A. 69, pp 1200~1203.

Zuckerwar, A.J., 1978, "Theoretical Response of Condenser Microphone," J.A.S.A. 64, pp 1278~1285.